Journal of
Materials Chemistry B

PAPER

View Article Online
View Journal | View Issue

Cite this: J. Mater. Chem. B, 2015, 3, 3324

Anchoring effects of surface chemistry on gold nanorods: modulating autophagy†

Shengliang Li,*[ab] Chunqiu Zhang,*[a] Weipeng Cao,[a] Benyu Ma,[c] Xiaowei Ma,[a] Shubin Jin,[a] Jinchao Zhang,[d] Paul C. Wang,[ef] Feng Li‡[b] and Xing-Jie Liang‡[a]

Received 13th January 2015,
Accepted 13th March 2015

DOI: 10.1039/c5tb00076a

www.rsc.org/MaterialsB

Gold nanorods (Au NRs) have been receiving extensive attention owing to their extremely attractive properties which make them suitable for various biomedical applications. Au NRs could induce nanotoxicity, but this problem could be turned into therapeutic potential through tuning autophagy. However, the autophagy-inducing activity and mechanism of Au NRs is still unclear. Here we showed that surface chemical modification can tune the autophagy-inducing activity of Au NRs in human lung adenocarcinoma A549 cells. CTAB-coated Au NRs induce remarkable levels of autophagy activity as evidenced by LC3-II conversion and p62 degradation, while PSS- and PDDAC-coated Au NRs barely induce autophagy. More importantly, we also demonstrated that the AKT-mTOR signaling pathway was responsible for CTAB-coated Au NRs-induced autophagy. We further showed that CTAB-coated Au NRs also induce autophagy in human fetal lung fibroblast MRC-5 cells in a time-dependent manner. This study unveils a previously unknown function for Au NRs in autophagy induction, and provides a new insight for designing surface modifications of Au NRs for biomedical applications.

Introduction

Owing to their unique properties, which depend on their shape, size, and aspect ratio, nanomaterials have attracted intense interest from scientists as therapeutic and diagnostic agents.[1–3] Gold nanorods (Au NRs) are one of most promising nanomaterials because their size, aspect ratio (ratio of length to diameter) and coating can all be easily controlled. Their applications in the biomedical field include cell and animal imaging, drug and gene delivery, and therapy and diagnosis in many diseases.[4–8] The most convenient synthesis method for Au NRs is the seed-mediated method using cetyltrimethylammonium bromide (CTAB), and CTAB is a well-known toxic cationic surfactant. Consequently the CTAB-Au NRs should be further coated by negatively charged PSS, positively charged PDDAC and PEG for biomedical applications. Recent studies have reported preliminary research into the intracellular localization, uptake and cytotoxicity of Au NRs in cells and whole animals. Qiu *et al.* showed that the aspect ratio and surface chemistry mediated the cellular uptake and cytotoxicity of Au NRs.[9] In addition, Wang *et al.* demonstrated that Au NRs can be selectively targeted to mitochondria and induce cell death for cancer therapy.[10] Our previous studies also indicated that the penetration and thermotherapy efficacy of Au NRs were determined by surface chemistry in multicellular tumor spheroids.[11] However, the mechanism of cell death induced by Au NRs is still unclear, and further study of the cell death mechanism is urgently needed before Au NRs are widely used in clinical studies.

Autophagy is a lysosome-based degradation process by which eukaryotic cells self-digest long-lived proteins and dysfunctional organelles, and thereby maintain intracellular homeostasis. Autophagy also plays an essential role in a variety of human diseases, including cancer, neurodegenerative disorders and infectious diseases.[12–14] In general, autophagy is regarded as a prosurvival mechanism. However, increasing evidence demonstrates that autophagy plays a key role in cell death.[15–17] Nanomaterials have been suggested to play different roles in autophagy and cell death due to their specific properties.[18,19] Recently, several studies have demonstrated that autophagy can be induced by a variety of nanomaterials, including quantum dots (QDs), polyamidoamine (PAMAM), single-walled carbon

[a] Chinese Academy of Sciences Key Lab for Biological Effects of Nanomaterials and Nanosafety, National Center for Nanoscience and Technology, No. 11, First North Road, Zhongguancun, 100190 Beijing, P. R. China. E-mail: liangxj@nanoctr.cn
[b] Department of Neurobiology and Anatomy, Zhongshan School of Medicine, Sun Yat-sen University, Guangzhou, China. E-mail: lifeng@mail.sysu.edu.cn
[c] The State Key Laboratory of Biomembrane and Membrane Biotechnology, Tsinghua-Peking Center for Life Sciences, School of Life Sciences, Tsinghua University, Beijing 100084, China
[d] College of Chemistry & Environmental Science, Chemical Biology Key Laboratory of Hebei Province, Hebei University, Baoding, P. R. China
[e] Laboratory of Molecular Imaging, Department of Radiology, Howard University, Washington, D.C. 20060, USA
[f] Fu Jen Catholic University, Taipei 24205, Taiwan

† Electronic supplementary information (ESI) available. See DOI: 10.1039/c5tb00076a

‡ These authors contributed equally to this work.

nanotubes (SWNTs) and lanthanide-based nanocrystals.[20–25] Our previous results show that gold nanoparticles can block autophagy in a size-dependent manner by increasing the lysosomal pH. In this work, we investigated the effect of Au NRs with different surface coatings on autophagy activity, and analyzed the underlying mechanisms and signaling pathway involved in Au NRs-induced autophagy.

Results and discussion

Synthesis and characterization of Au NRs

In order to investigate the surface chemistry-dependent induction of autophagy activity by Au NRs, we synthesized Au NRs with three different polymer coatings: cetyltrimethylammonium bromide (CTAB), polystyrene sulfonate (PSS) and poly(diallyldimethylammonium chloride) (PDDAC) as described in the Experimental section. CTAB, PSS and PDDAC are frequently used as model polymer coatings in Au NRs. As shown in Fig. 1a, the morphology and size of the Au NRs were measured and statistically analyzed based on TEM images. The aspect ratio of all Au NRs was 4, and the mean size of the Au NRs was 55 nm × 14 nm (length × diameter). The UV-Vis-NIR absorption spectra showed that the maximum absorption peaks were close to 808 nm, and the visible absorption spectrum was correlated with the shape, size, monodispersion and surface stabilization of the Au NRs (Fig. 1b). Zeta potential is usually used to predict the surface charge and stability of nanomaterials in solution. We measured the zeta potentials and found that the CTAB-coated Au NRs and the PDDAC-coated Au NRs were positively charged, whereas the PSS-coated Au NRs were negatively charged (Fig. 1c–e). This result is consistent with previous studies on coated Au NRs under the same conditions. It has been previously reported that the size and zeta potential of Au NRs are critical for the nonspecific adsorption of serum proteins onto the surface, and the presence of these proteins on the surface of the nanoparticles is related to the cellular uptake and cytotoxicity.[9] We further examined the zeta potential of the surface-coated Au NRs after incubating them with DMEM containing 10% fetal bovine serum for 2 hours. The surface charges of all the Au NRs immediately became negative, as we expected (Fig. S1 in ESI†). Thus the results of the following autophagy studies most likely depend on the surface coating of the Au NRs instead of their zeta potential.

Autophagic cell death induced by CTAB-coated Au NRs

In order to understand the mechanism of cell death induced by Au NRs, we first examined the cytotoxicity of CTAB-, PSS- and PDDAC-coated Au NRs using the autophagy inhibitor 3-methyladenine (3-MA). Starvation, the most widely used inducer of autophagy, was employed as a positive control. The results showed that 70 pM Au NRs exhibited coating-dependent toxicity to human lung adenocarcinoma A549 cells (Fig. 2a). The CTAB-coated Au NRs have notable cytotoxicity, but when further coated with PSS and PDDAC, the cytotoxicity of the Au NRs decreased greatly to negligible levels. Interestingly, we observed that the cytotoxicity induced by CTAB-coated Au NRs could be rescued by treatment with 3-MA, suggesting that CTAB-coated Au NRs likely induced cell death *via* autophagy.

To further confirm our hypothesis that CTAB-coated Au NRs induced cell death through autophagy, we used TEM to examine the formation of autophagosomes, which are key intermediate vesicles in the autophagy pathway. TEM imaging revealed that treatment with CTAB-coated Au NRs significantly increased autophagosome formation in A549 cells (Fig. 2b), compared to those treated with PSS- and PDDAC-coated Au NRs. We next examined the conversion of the autophagy-related protein

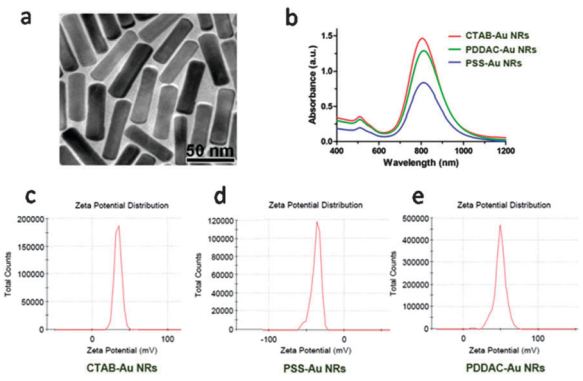

Fig. 1 Characterization of Au NRs. (a) TEM image of the CTAB-coated Au NRs. (b) Representative UV-Vis-NIR absorption spectra of CTAB-coated Au NRs, PSS-coated Au NRs and PDDAC-coated Au NRs. (c–e) Zeta potential distribution of Au NRs coated with CTAB (c), PSS (d) and PDDAC (e).

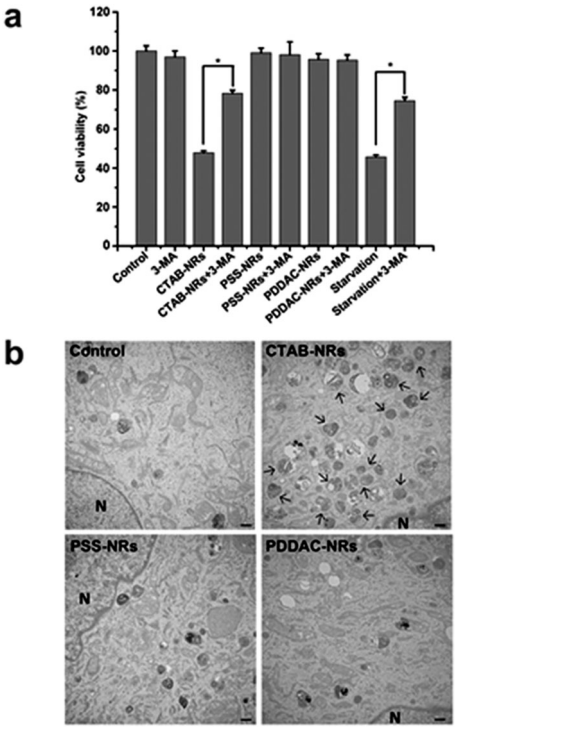

Fig. 2 Autophagic features induced by Au NRs. (a) Cell death detection after treatment with Au NRs alone, or Au NRs plus the autophagy inhibitor 3-MA. (b) TEM images of autophagosomes in A549 cells treated with Au NRs for 4 hours. Black arrows, autophagosomes. Scale bar, 500 nm.

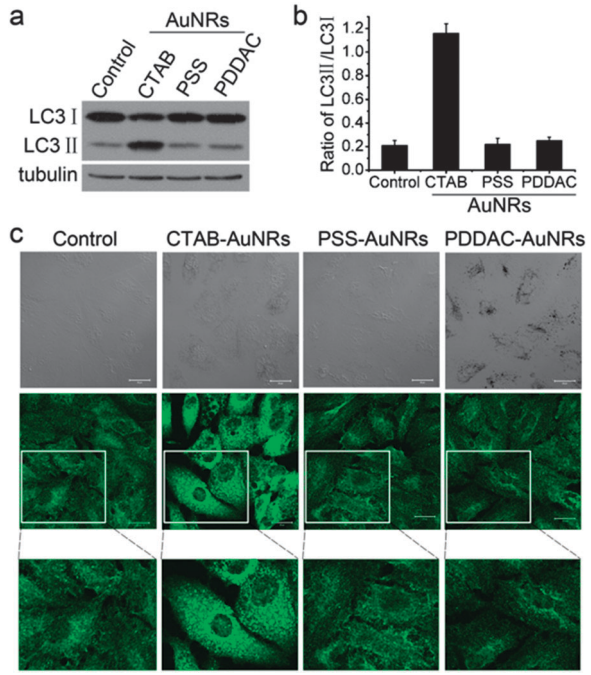

Fig. 3 Changes in LC3 distribution induced by Au NR treatment. (a) Western blotting of LC3 in A549 cells that were untreated (control) or treated with Au NRs for 4 h. (b) Statistical analysis of the LC3-II band intensity relative to that of LC3-I in (a). (c) Confocal microscopy images of the formation of endogenous LC3-positive dots in A549 cells treated with different surface-coated Au NRs for 4 h. Scale bar, 20 μm.

microtubule-associated protein 1 light chain 3 (LC3).[26] LC3 has two isoforms, LC3-I, which is cytosolic, and LC3-II, which associates with autophagosomal membranes. Autophagy is characterized by an increase in LC3-II protein and LC3-positive puncta. We analyzed the expression of LC3 by western blotting and found that CTAB-coated Au NRs induced a remarkable increase in LC3-II expression compared to the control, while PSS- and PDDAC-coated Au NRs did not change the LC3-II/LC3-I ratio (Fig. 3a and b). Consistently, CTAB-coated Au NRs but not PSS- and PDDAC-coated Au NRs increased LC3 puncta formation (Fig. 3c). Moreover, we also observed that the number of PDDAC-coated Au NRs in cells was much greater than that of CTAB- or PSS-coated Au NRs. These results indicated that the level of Au NR uptake was not related to the level of autophagy induction. In addition, CTAB-coated Au NRs also induce accumulation of LC3-II in a HeLa cell line which stably expresses GFP-tagged LC3 (Fig. S2, ESI†). To confirm these results, human fetal lung fibroblast (MRC-5) cells, a normal cell line, was chose to analyze LC3-II conversion after treatment with CTAB-coated Au NRs (Fig. S3, ESI†). CTAB-coated Au NRs also induce autophagy in MRC-5 cells in a time-dependent manner. Taken together, these data demonstrate that CTAB-coated Au NRs can influence the autophagy process.

Au NRs have no effect on the function of lysosomes

Autophagosome accumulation and the enhancement of the LC3-II/LC3-I ratio may be due to inhibition or induction of autophagy.[27] It is well known that lysosome function, especially the internal pH, plays vital roles in maintaining cellular processes,

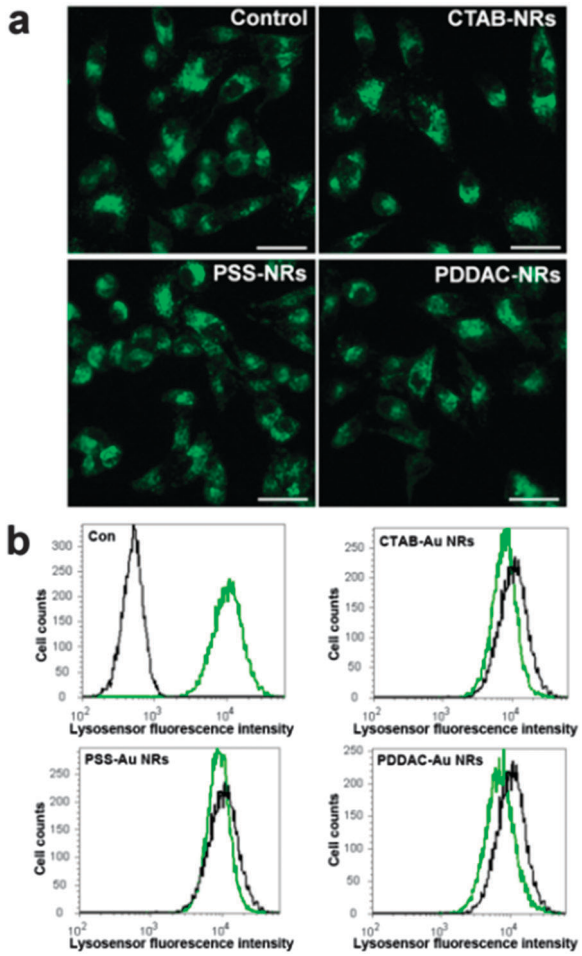

Fig. 4 Effect of different surface-coated Au NRs on lysosome pH. (a) Representative fluorescence images of A549 cells treated with different surface-coated Au NRs for 4 h, then exposed for 30 min to 1 μM LysoSensor Green DND-189 (scale bar, 50 μm). (b) FACS analysis of cells stained with LysoSensor Green DND-189.

including autophagy. LysoSensor Green DND-189 shows an acidification-dependent increase in fluorescence intensity, which allows us to monitor pH changes in lysosomes.[28,29] Our previous study showed that gold nanoparticles decreased the alkalinization of lysosomes and therefore inhibited autophagy in a size-dependent manner.[30] In order to examine whether Au NRs can affect lysosome pH, A549 cells were labeled with LysoSensor Green DND-189 dye after treatment with different Au NRs. Confocal microscopy analysis demonstrated that lysosome pH was unaffected in Au NR-treated cells (Fig. 4a). Flow cytometry analysis also confirmed this result (Fig. 4b and Fig. S4, ESI†). These results indicate that CTAB-, PSS- and PDDAC-coated Au NRs have no effect on lysosome pH and do not influence the autophagy process by this mechanism.

The AKT-mTOR signaling pathway is involved in CTAB-coated Au NR-induced autophagy

To further distinguish whether the main effect of CTAB-coated Au NRs is on autophagy induction or the blockage of autophagic flux, the ratio of LC3-II/LC3-I was checked in the presence and

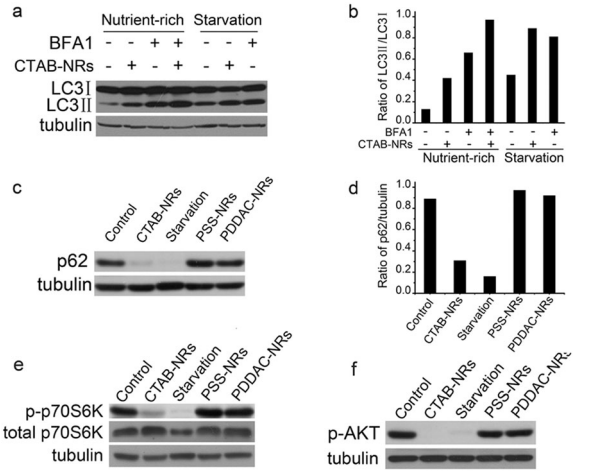

Fig. 5 Au NRs induce autophagy through the AKT-mTOR signaling pathway. (a) Western blotting of LC3 in A549 cells that were treated with CTAB-Au NRs under nutrient-rich or starvation conditions for 4 h with or without BFA1. (b) Statistical analysis of the LC3-II/LC3-I band density ratio in (a). (c) The degradation of p62 was detected by Western blotting. (d) Statistical analysis of the p62/tubulin band density ratio in (c). (e) Effect of Au NRs on the level of phospho-p70S6 kinase (p-p70S6K). Cells starved or treated with Au NRs for 4 h were analyzed with anti-p70S6K and anti-phospho-p70S6K antibodies. (f) Western blotting analysis of Au NR-treated and untreated control cells probed with anti-phospho-AKT antibody.

absence of a lysosome degradation inhibitor, bafilomycin A1 (BFA1). It was found that BFA1 further increased the CTAB-coated Au NR-induced conversion of LC3-II (Fig. 5a and b). This result indicates that the CTAB-coated Au NRs themselves actually induced autophagy. p62 (also known as SQSTM1/sequestome1), a substrate that is preferentially degraded by autophagy, was also monitored by western blotting analysis.[31] As shown in Fig. 5c and d, starvation induced rapid down-regulation of p62. CTAB-coated Au NRs also caused marked down-regulation of p62, while PSS- and PDDAC-coated Au NRs had no effect on p62 protein level. These data suggest that CTAB-coated Au NRs promote autophagy to accelerate p62 turnover through blocking autophagic flux. In mammalian cells, autophagy is regulated by several classical signaling pathways, most of which involve the inhibition of a serine/threonine protein kinase, mammalian target of rapamycin (mTOR).[32,33] The mTOR protein exists in a phosphorylated form and suppresses autophagy under normal conditions, but when the level of phosphorylated mTOR is down-regulated, such as during starvation, autophagy is up-regulated. To test whether CTAB-coated Au NRs induced-autophagy occurred *via* inhibition of mTOR activity, the level of phosphorylated p70 S6 kinase (p-p70S6K), an indicator for mTOR activity, was examined by western blotting analysis. It was found that both CTAB-coated Au NRs and starvation significantly decreased the level of (p-p70S6K), while PSS- and PDDAC-coated Au NRs had no effect on the expression of p-p70S6K (Fig. 5e). This demonstrated that CTAB-coated Au NRs induced autophagy through down-regulation of mTOR activity. Previous studies have shown that the effect of mTOR on autophagy can be regulated by the PI3K-AKT-TSC1/2 pathway.[34] To further understand the signaling pathway involved in CTAB-coated Au NR-induced autophagy, we examined phosphorylated AKT, a vital marker upstream of the mTOR pathway.[35] As shown in Fig. 5f, the phosphorylated AKT level was significantly decreased when cells were incubated with CTAB-coated Au NRs, and starvation caused similar reductions. PSS- and PDDAC-coated Au NRs were analyzed under the same conditions, and had no effect on the levels of phosphorylated AKT, as we expected. Together, these results revealed that CTAB-coated Au NRs induced autophagy through the AKT-mTOR signaling pathway, while other surface coatings did not induce autophagy.

Conclusions

Accumulating evidence shows that Au NRs cause cell death for cancer therapy, however, the molecular mechanism to trigger cytotoxicity is poorly understood. As illustrated in Fig. 6, we have provided compelling evidence that CTAB-coated Au NRs promote autophagy while other surface-modifying polymers did not cause an obvious autophagy process, indicating that the autophagy-inducing activity of Au NRs is tuned by surface chemistry. Meanwhile, CTAB-coated Au NRs also induce autophagy in human fetal lung fibroblast MRC-5 cells in a time-dependent manner. Furthermore, we demonstrated that the AKT-mTOR signaling pathway is involved in the induction of autophagy by CTAB-coated Au NRs. Herein, this study unveils a previously unknown function for CTAB-coated Au NRs in autophagy induction and provides guidance for the rational design of surface coatings for nanoparticles in biomedical applications and pharmaceutical therapy.

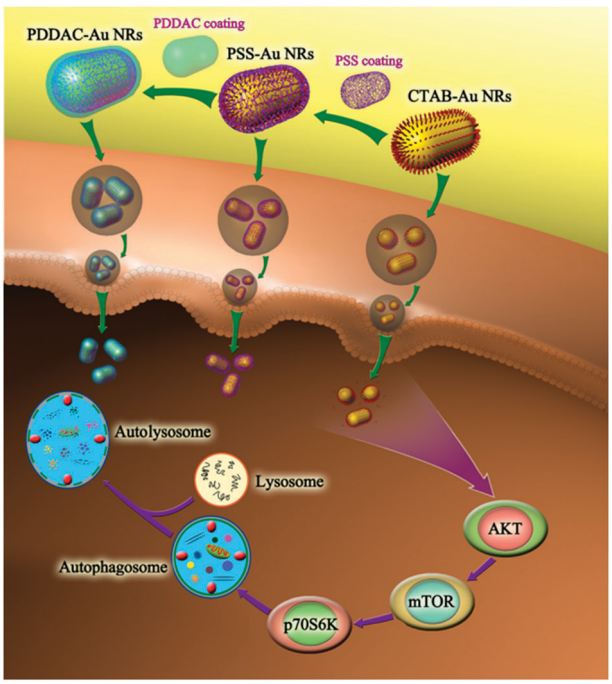

Fig. 6 Schematic illustration of the mechanism and signaling pathways in autophagy induced by CTAB-Au NRs.

Experimental section

Materials and antibodies

Dulbecco's Modified Eagle's Medium (DMEM) and fetal bovine serum (FBS) were obtained from Hyclone (Logan, UT, USA). Cetyltrimethylammonium bromide (CTAB), hydrogen tetrachloroaurate(III) trihydrate ($HAuCl_4 \cdot 3H_2O$), silver nitrate ($AgNO_3$), L-ascorbic acid, and sodium borohydride ($NaBH_4$) were purchased from Alfa Aesar. Poly(sodium-*p*-styrenesulfate) (PSS, molecular weight: 70 000) and poly (diallyldimethyl ammonium chloride) (PDDAC, 20%) were obtained from Aldrich. Lysosensor green DND-189 (L-7535) was purchased from Invitrogen. The polyclonal anti-LC3 antibody (NB100-2220) was obtained from MBL. The anti-p62 antibody was purchased from MBL. The monoclonal anti-p70S6K (#2708) and anti-phospho-p70S6K antibodies (#9206) were obtained from Cell Signaling Technology. Deionized water (18.2 MΩ cm^{-1}) produced by a Milli-Q system (Millipore Co., USA) was used in all the experiments. Unless specified, all of the commercial products were used without further purification.

CTAB-coated Au NRs

As described previously, the CTAB-coated Au NRs were synthesized by seed-mediated growth.[36,37] First, the CTAB-capped Au seeds were obtained by chemical reduction of $HAuCl_4$ with $NaBH_4$: 7.5 ml CTAB (0.1 M) was mixed with 100 μl $HAuCl_4$ (24 mM) and diluted with water to 9.4 ml. Then, 0.6 ml ice-cold $NaBH_4$ (0.01 M) was freshly prepared and added while stirring magnetically. After 2 min of vigorous stirring, the seed solution was kept at room temperature (25 °C) and used within 2–5 h. Second, the Au NR growth solution, consisting of 100 ml CTAB (0.1 M), 2 ml $HAuCl_4$ (24 mM), 2 ml H_2SO_4 (0.5 M), a certain amount of $AgNO_3$ (10 mM), and 800 μl ascorbic acid (0.1 M) was prepared. The amount of Ag ions added was used to control the aspect ratio of the Au NRs. Afterwards, 240 μl of seed solution was added to the above growth solution to initiate the growth of the Au NRs. The reaction was stopped after 12 h and the outcome was centrifuged at 8000 rpm for 10 min. The precipitates were collected and re-suspended in deionized water. Au NRs with an aspect ratio of 4 were obtained.

Polyelectrolyte-coated Au NRs

The preparation of multilayer polyelectrolyte-coated Au NRs was performed *via* a layer-by-layer approach according to previous references.[38,39] The multilayer polyelectrolyte-coated Au NRs were synthesized by sequentially coating negatively charged PSS and positively charged PDDAC onto the as-synthesized CTAB-coated Au NRs. For PSS coating, 12 ml Au NRs were centrifuged at 12 000 rpm for 10 min, and the precipitate was dispersed in 12 ml of 2 mg ml^{-1} PSS aqueous solution (containing 6 mM NaCl). The solution was stirred magnetically for 3 h. Afterwards, this solution was centrifuged at 12 000 rpm for 10 min, and the precipitate was redispersed in water. For further coating with PDDAC, a similar procedure was applied to the PSS-coated Au NRs.

Characterization of Au NRs

UV-Vis-NIR absorbance, transmission electron microscopy (TEM) and dynamic light scattering (DLS) were used for characterization of the optical properties, size and zeta potential of the particles. The UV-Vis-NIR absorption spectra were measured with a Lambda 950 UV/Vis/NIR spectrophotometer (Perkin-Elmer, USA). The size and morphology of the Au NRs was determined using a Tecnai G220 STWIN transmission electron microscope (FEI Company, Philips, Netherlands) with 200 kV acceleration voltage. The zeta-potential distribution of the Au NRs was measured by a Zetasizer Nano ZS (Malvern, England), at 25 °C.

CCK-8 assay

The human lung adenocarcinoma A549 cell line was purchased from ATCC, and cultured in DMEM supplemented with 10% FBS and 100 U ml^{-1} penicillin/streptomycin at 37 °C in a 5% CO_2 incubator at 95% humidity. A549 cells were seeded at a density of 5×10^3 cells per well in 96-well plates in culture medium and incubated overnight. The cells were then pre-treated with or without 3-MA for 4 h and the medium was then replaced with 100 μl of 70 pM Au NRs, Au NRs plus 3-MA or 3-MA. After a further incubation period of 24 h, cytotoxicity assays were performed using CCK-8 Kits (Dojindo Molecular Technologies, Tokyo, Japan). Absorbance was detected at 450 nm with a TECAN Infinite M200 microplate reader (Tecan, Durham, USA). All experiments were conducted in triplicate.

Transmission electron microscopy analysis

3×10^5 A549 cells were seeded in 33 mm dishes overnight, then incubated with 70 pM Au NRs for 4 h. The cells were fixed in 2.5% glutaraldehyde in 0.01 M PBS (pH 7.4) for 10 min at room temperature. The fixed cells were then embedded, sectioned and double stained with uranyl acetate and lead citrate for observation under the transmission electron microscope (H-7650B).

Evaluation of lysosomal acidity

A549 cells were collected from growth media after treating with 70 pM Au NRs for 4 h and washed three times with 0.01 M PBS. The cells were incubated for 30 min under growth conditions with 500 μl of prewarmed medium containing 2 μmol L^{-1} LysoSensor Green DND-189 dye (Invitrogen). After washing, the cells were resuspended in 0.01 M PBS and immediately analyzed by an Attune® acoustic focusing cytometer (Applied Biosystems, Life Technologies, Carlsbad, CA). The cytometer was purchased jointly with the Nanotechnology lab for bioapplications, and was installed by Life Technologies Corp. in the National Center for Nanoscience and Technology, China. The green fluorescence was collected within 1 min from a population of 20 000 cells.

Immunofluorescence analysis

Immunofluorescence analysis was performed as described previously.[40] Cells were grown in six-well plates on glass coverslips and treated with 70 pM Au NRs for 4 h. Before incubation with antibodies, cells were fixed for 30 min with 4% paraformaldehyde at room temperature, permeabilized for 10 min with

0.2% Triton X-100 (Sigma) and blocked for 2 h in 10% horse serum albumin. Incubation overnight at 4 °C with the primary antibody was followed by the secondary antibody for 3 h at room temperature. Endogenous LC3 was detected with anti-LC3 antibodies. Confocal laser scanning was done on a Zeiss LSM 710 Laser Scanning Microscope.

Western blotting

After incubating with 70 pM Au NRs for 4 h, A549 cells were lysed in lysis buffer, denatured at 100 °C for 10 min and then the proteins were separated by SDS-PAGE before transferring to PVDF membranes. Membranes were blocked for 1 h with 0.01 M PBS/0.05% Tween/5% milk. The PVDF membranes were incubated with the primary antibody at 4 °C overnight, washed in TBST, and detected by a horseradish peroxidase-conjugated secondary antibody at room temperature for 1 hour followed by treatment with the ECL detection system. Quantitative analysis was calculated using AlphaEaseFC software.

Statistical analysis

All data are presented as the mean ± standard deviation (SD). Differences between groups were analyzed by a one-way analysis of variance (ANOVA) and *t*-test using the SPSS software package. In all statistical analyses, $p < 0.05$ was regarded as statistically significant.

Acknowledgements

This work was supported by the Chinese Natural Science Foundation project (No. 30970784, 81171455 and 81271476), a National Distinguished Young Scholars grant (31225009) from the National Natural Science Foundation of China, the National Key Basic Research Program of China (2009CB930200), the Chinese Academy of Sciences (CAS) ''Hundred Talents Program'' (07165111ZX), the CAS Knowledge Innovation Program and the State High-Tech Development Plan (2012AA020804). This work was also supported in part by NIH/NIMHD 8 G12 MD007597, and USAMRMC W81XWH-10-1-0767 grants. The authors also appreciate the support by the ''Strategic Priority Research Program'' of the Chinese Academy of Sciences, Grant No. XDA09030301 and support by the external cooperation program of BIC, Chinese Academy of Science, Grant No. 121D11KYSB20130006.

Notes and references

1 Y. Xia, Nanomaterials at work in biomedical research, *Nat. Mater.*, 2008, **7**, 758.
2 E. Lavik and H. von Recum, The role of nanomaterials in translational medicine, *ACS Nano*, 2011, **5**, 3419.
3 M. Srikanth and J. A. Kessler, Nanotechnology-novel therapeutics for CNS disorders, *Nat. Rev. Neurol.*, 2012, **8**, 307.
4 D. P. Yang and D. X. Cui, Advances and prospects of gold nanorods, *Chem. – Asian J.*, 2008, **3**, 2010.
5 W. I. Choi, A. Sahu, Y. H. Kim and G. Tae, Photothermal cancer therapy and imaging based on gold nanorods, *Ann. Biomed. Eng.*, 2012, **40**, 534.
6 X. Huang, I. H. El-Sayed, W. Qian and M. A. El-Sayed, Cancer cell imaging and photothermal therapy in the near-infrared region by using gold nanorods, *J. Am. Chem. Soc.*, 2006, **128**, 2115.
7 A. K. Salem, P. C. Searson and K. W. Leong, Multifunctional nanorods for gene delivery, *Nat. Mater.*, 2003, **2**, 668.
8 X. H. Huang, S. Neretina and M. A. El-Sayed, Gold Nanorods: From Synthesis and Properties to Biological and Biomedical Applications, *Adv. Mater.*, 2009, **21**, 4880.
9 Y. Qiu, Y. Liu, L. Wang, L. Xu, R. Bai, Y. Ji, X. Wu, Y. Zhao, Y. Li and C. Chen, Surface chemistry and aspect ratio mediated cellular uptake of Au nanorods, *Biomaterials*, 2010, **31**, 7606.
10 L. Wang, Y. Liu, W. Li, X. Jiang, Y. Ji, X. Wu, L. Xu, Y. Qiu, K. Zhao, T. Wei, Y. Li, Y. Zhao and C. Chen, Selective targeting of gold nanorods at the mitochondria of cancer cells: implications for cancer therapy, *Nano Lett.*, 2011, **11**, 772.
11 S. Jin, X. Ma, H. Ma, K. Zheng, J. Liu, S. Hou, J. Meng, P. C. Wang, X. Wu and X. J. Liang, Surface chemistry-mediated penetration and gold nanorod thermotherapy in multicellular tumor spheroids, *Nanoscale*, 2012, **5**, 143.
12 N. Mizushima, B. Levine, A. M. Cuervo and D. J. Klionsky, Autophagy fights disease through cellular self-digestion, *Nature*, 2008, **451**, 1069.
13 B. Levine, N. Mizushima and H. W. Virgin, Autophagy in immunity and inflammation, *Nature*, 2011, **469**, 323.
14 D. C. Rubinsztein, P. Codogno and B. Levine, Autophagy modulation as a potential therapeutic target for diverse diseases, *Nat. Rev. Drug Discovery*, 2012, **11**, 709.
15 Y. Tsujimoto and S. Shimizu, Another way to die: autophagic programmed cell death, *Cell Death Differ.*, 2005, **12**, 1528.
16 D. Denton, S. Nicolson and S. Kumar, Cell death by autophagy: facts and apparent artefacts, *Cell Death Differ.*, 2012, **19**, 875.
17 G. Kroemer and B. Levine, Autophagic cell death: the story of a misnomer, *Nat. Rev. Mol. Cell Biol.*, 2008, **9**, 1004.
18 F. Wang, M. G. Bexiga, S. Anguissola, P. Boya, J. C. Simpson, A. Salvati and K. A. Dawson, *Nanoscale*, 2013, **5**, 10868.
19 J. A. Kim, C. Åberg, G. de Cárcer, M. Malumbres, A. Salvati and K. A. Dawson, *ACS Nano*, 2013, **7**, 7483.
20 O. Seleverstov, O. Zabirnyk, M. Zscharnack, L. Bulavina, M. Nowicki, J. M. Heinrich, M. Yezhelyev, F. Emmrich, R. O'Regan and A. Bader, Quantum dots for human mesenchymal stem cells labeling. A size-dependent autophagy activation, *Nano Lett.*, 2006, **6**, 2826.
21 C. Li, H. Liu, Y. Sun, H. Wang, F. Guo, S. Rao, J. Deng, Y. Zhang, Y. Miao, C. Guo, J. Meng, X. Chen, L. Li, D. Li, H. Xu, H. Wang, B. Li and C. Jiang, PAMAM nanoparticles promote acute lung injury by inducing autophagic cell death through the Akt-TSC2-mTOR signaling pathway, *J. Mol. Cell Biol.*, 2009, **1**, 37.
22 H. L. Liu, Y. L. Zhang, N. Yang, Y. X. Zhang, X. Q. Liu, C. G. Li, Y. Zhao, Y. G. Wang, G. G. Zhang, P. Yang, F. Guo,

Y. Sun and C. Y. Jiang, A functionalized single-walled carbon nanotube-induced autophagic cell death in human lung cells through Akt-TSC2-mTOR signaling, *Cell Death Dis.*, 2011, **2**, e159.

23 Y. Zhang, F. Zheng, T. Yang, W. Zhou, Y. Liu, N. Man, L. Zhang, N. Jin, Q. Dou, Y. Zhang, Z. Li and L. P. Wen, Tuning the autophagy-inducing activity of lanthanide-based nanocrystals through specific surface-coating peptides, *Nat. Mater.*, 2012, **11**, 817.

24 J. J. Li, D. Hartono, C. N. Ong, B. H. Bay and L. Y. Yung, Autophagy and oxidative stress associated with gold nanoparticles, *Biomaterials*, 2010, **31**, 5996.

25 S. Hussain, F. Al-Nsour, A. B. Rice, J. Marshburn, B. Yingling, Z. Ji, J. I. Zink, N. J. Walker and S. Garantziotis, Cerium dioxide nanoparticles induce apoptosis and autophagy in human peripheral blood monocytes, *ACS Nano*, 2012, **6**, 5820.

26 Y. Kabeya, N. Mizushima, T. Ueno, A. Yamamoto, T. Kirisako, T. Noda, E. Kominami, Y. Ohsumi and T. Yoshimori, LC3, a mammalian homologue of yeast Apg8p, is localized in autophagosome membranes after processing, *EMBO J.*, 2000, **19**, 5720.

27 A. Kuma, M. Matsui and N. Mizushima, LC3, an autophagosome marker, can be incorporated into protein aggregates independent of autophagy: caution in the interpretation of LC3 localization, *Autophagy*, 2007, **3**, 323.

28 J. Han and K. Burgess, Fluorescent indicators for intracellular pH, *Chem. Rev.*, 2010, **110**, 2709.

29 B. Poole and S. Ohkuma, Effect of weak bases on the intralysosomal pH in mouse peritoneal macrophages, *J. Cell Biol.*, 1981, **90**, 665.

30 X. Ma, Y. Wu, S. Jin, Y. Tian, X. Zhang, Y. Zhao, L. Yu and X. J. Liang, Gold nanoparticles induce autophagosome accumulation through size-dependent nanoparticle uptake and lysosome impairment, *ACS Nano*, 2011, **5**, 8629.

31 G. Bjørkøy, T. Lamark, A. Brech, H. Outzen, M. Perander, A. Overvatn, H. Stenmark and T. Johansen, p62/SQSTM1 forms protein aggregates degraded by autophagy and has a protective effect on huntingtin-induced cell death, *J. Cell Biol.*, 2005, **171**, 603.

32 L. Yu, C. K. McPhee, L. Zheng, G. A. Mardones, Y. Rong, J. Peng, N. Mi, Y. Zhao, Z. Liu, F. Wan, D. W. Hailey, V. Oorschot, J. Klumperman, E. H. Baehrecke and M. J. Lenardo, Termination of autophagy and reformation of lysosomes regulated by mTOR, *Nature*, 2010, **465**, 942.

33 C. H. Jung, S. H. Ro, J. Cao, N. M. Otto and D. H. Kim, mTOR regulation of autophagy, *FEBS Lett.*, 2010, **584**, 1287.

34 Y. P. Yang, Z. Q. Liang, Z. L. Gu and Z. H. Qin, Molecular mechanism and regulation of autophagy, *Acta Pharmacol. Sin.*, 2005, **26**, 1421.

35 C. Mammucari, S. Schiaffino and M. Sandri, Downstream of Akt: FoxO3 and mTOR in the regulation of autophagy in skeletal muscle, *Autophagy*, 2008, **4**, 524.

36 M. Liu and P. Guyot-Sionnest, Mechanism of silver(I)-assisted growth of gold nanorods and bipyramids, *J. Phys. Chem. B*, 2005, **109**, 22192.

37 T. K. Sau and C. J. Murphy, Seeded high yield synthesis of short Au nanorods in aqueous solution, *Langmuir*, 2004, **20**, 6414.

38 H. Ding, K. T. Yong, I. Roy, H. E. Pudavar, W. C. Law, E. J. Bergey and P. N. Prasad, Gold nanorods coated with multilayer polyelectrolyte as contrast agents for multimodal imaging, *J. Phys. Chem. C*, 2007, **111**, 12552.

39 A. M. Gole and C. J. Murphy, Polyelectrolyte-coated gold nanorods: synthesis, characterization and immobilization, *Chem. Mater.*, 2005, **17**, 1325.

40 J. S. Guan, Z. Z. Xu, H. Gao, S. Q. He, G. Q. Ma, T. Sun, L. H. Wang, Z. N. Zhang, I. Lena, I. Kitchen, R. Elde, A. Zimmer, C. He, G. Pei, L. Bao and X. Zhang, Interaction with vesicle luminal protachykinin regulates surface expression of delta-opioid receptors and opioid analgesia, *Cell*, 2005, **122**, 619.

